Circulating circular RNA hsa_circ_0023179 acts as a diagnostic biomarker for non-small-cell lung cancer detection

Shaoqing Ju (jsq814@hotmail.com)
Affiliated Hospital of Nantong University

Qi Zhang
Nantong University

Shiyi Qin
Nantong University

Chunlei Peng
Affiliated Tumor Hospital of Nantong University

Yupeng Liu
Affiliated Tumor Hospital of Nantong University

Yuejiao Huang
Affiliated Hospital of Nantong University

Research Article

Keywords: non-small-cell lung cancer, hsa_circ_0023179, biomarker, diagnosis, prognosis

Posted Date: April 12th, 2022

DOI: https://doi.org/10.21203/rs.3.rs-1535586/v1

Abstract

Background: Lung cancer, the most prevalent cancer-related death worldwide, still lacks the means for early diagnosis. Because of the unique properties of the loop that make it stable in body fluids, circular RNAs (circRNAs) as a biomarker becomes a possibility. This research purposed to explore whether hsa_circ_0023179 can be applied as a possible biomarker for the early diagnosis and prognosis of non-small cell lung cancer (NSCLC).

Methods: hsa_circ_0023179 was screened by high-throughput sequencing of three pairs of NSCLC tissues and their surrounding tissues. Agarose gel electrophoresis (AGE), Sanger sequencing, exonuclease digestion assay, and actinomycin D were used to affirm the molecular properties of circRNA. Precision determination was performed by placement at room temperature and multiple freeze-thawing test for methodological evaluation. The expression of hsa_circ_0023179 in tissues, serum, and cells was determined by quantitative real-time polymerase chain reaction (qRT-PCR) to establish the receiver operating characteristic (ROC) curve to assess the diagnostic efficacy of hsa_circ_0023179.

Results: hsa_circ_0023179 conforms to the basic properties of circRNA, and the detection method of hsa_circ_0023179 has good stability and repeatability. Its expression was connected to histological type, TNM stage, lymph node metastasis, and distal metastasis in NSCLC tissues, serum, and cells. Compared with traditional tumor markers with higher sensitivity and specificity. A combined diagnosis can significantly improve the diagnostic value. The decrease in postoperative expression level suggests some potential for dynamic monitoring.

Conclusion: hsa_circ_0023179 might be a promising novel serum marker for the detection and prediction of NSCLC.

1. Introduction

Lung cancer is a type of malignant tumor originating from the bronchial or alveolar epithelium. According to global lung cancer data from 2020, lung cancer is the second most prevalent malignant tumor, with 2.21 million new cases and 1.7 million deaths reported (accessed on 18 February 2022) (Cancer, 2020), posing a serious threat to human survival and development. posing a serious threat to human survival and development. Meanwhile, lung cancer is the leading cause of death from malignant tumors in males and females in China (Sung et al., 2021). Lung cancer is histologically divided into small cell lung cancer (SCLC) and non-small cell lung cancer (NSCLC). NSCLC is the most aggressive form of lung cancer, accounting for more than 85 percent of all occurrences (Herbst, Morgensztern, & Boshoff, 2018). It can be subdivided into lung adenocarcinoma (LUAD), squamous cell carcinoma (LUSC), and large cell carcinoma (LCC) (Zhang, Li, Ji, & Fang, 2018). The primary treatment for lung cancer is surgery, followed by postoperative radiotherapy and chemotherapy, but the therapeutic effect is not ideal. The main reason is that about 60% of lung cancer patients have had distant metastasis at the time of initial diagnosis, lead to low survival rate. Therefore, we should focus more attention on prevention and early diagnosis.

CircRNAs are a new type of single-stranded RNAs with a covalent closed-loop structure widely present in the transcriptome of various species and tissues (Memczak et al., 2013). It is mainly produced by reverse splicing of precursor messenger RNAs (mRNAs). Unlike common linear RNAs (with 3’ and 5’ ends), they lack the terminal 5’ cap and 3’ poly(A) tail structures and have higher structural stability and conservation (Cai et al., 2022). Eukaryotic circular RNAs were found in the early 1990s and were considered results of error splicing or splicing intermediates (Cocquerelle, Mascrez, Hétuin, & Bailleul, 1993). Meanwhile, traditional RNA detection methods using electrophoresis or size mobility transfer tests could not detect circRNA molecules (Palcau et al., 2022). As a result, the study of circRNA has not been widely carried out until recent years. CEA, SCC, and Cyfra21-1 as several known tumor biomarkers of NSCLC, poor sensitivity and specificity prevent the early screening of NSCLC (Schiffman, Fisher, & Gibbs, 2015). Consequently, in recent years, extensive research has been devoted to finding tumor markers with higher diagnostic efficacy.

The emergence of liquid biopsy, a noninvasive diagnostic technique for tumors, marks a step forward in conquering tumors. Among them, the detection and quantification of circRNAs have received much attention (de Fraipont, Gazzeri, Cho, & Eymin, 2019). Although circRNA field is still in its infancy, several studies have confirmed the unique expression characteristics of circRNA and its great potential as a tumor marker (Arnaiz et al., 2019). Based on the current circRNA investigation and the significant challenges facing the diagnosis of NSCLC, we conducted this experiment. hsa_circ_0023179 notably upregulated in NSCLC was first identified by high-throughput sequencing. It turned out that hsa_circ_0023179 conforms to the basic properties of circRNA and has higher

sensitivity and specificity than conventional serum markers of NSCLC. We reasonably guessed its potential as a serum marker for NSCLC and conducted follow-up exploration.

2. Materials And Methods

2.1 Serum and Tissue Samples

Serum samples include 126 NSCLC patients, 36 patients with benign pulmonary diseases (BPDs) and 114 healthy donors, which were confirmed by Affiliated Hospital of Nantong University from 2016 to 2021. All participants did not receive preoperative radiotherapy, chemotherapy or other adjuvant therapy, and those with prior tumor history were excluded. The NSCLC tissue samples involved in this investigation were collected from the thoracic surgery of the Affiliated Hospital of Nantong University and the Affiliated Tumor Hospital of Nantong University. Tissues were collected within 30min after surgical resection, and normal tissues adjacent to the cancer were obtained more than 5cm from the tumor margin, placed in RNase-free cryopreservation tubes containing RNA fixatives at -80℃. Subject's informed consent and approval by the Ethics Committee of Affiliated Hospital of Nantong University (Ethics review report number: 2018-L055).

2.2 Cell Culture

Four human NSCLC cell lines (A549, NCI-H1299, NCI-H226, and SPC-A1) and normal bronchial epithelial cell lines (HBE) used in this experiment were purchased from the Shanghai Institute of Biological Sciences, Chinese Academy of Sciences (Shanghai, China). The cell culture medium was composed of RPMI-1640 (Corning, Manassas, VA) medium + 10% fetal bovine serum (FBS, Gibco, Grand Island, NY) + 1% Tri Antibody (Sheng Gong, Nantong, China) and placed in a humidified incubator (37°C, 5% CO_2). Log-phase cells with better growth were selected for the experiments.

2.3 Total RNA Extraction and Complementary DNA (cDNA) Synthesis

Total RNA was extracted from NSCLC cells, tissues, and serum using TRIzol reagent (Invitrogen, Karlsruhe, Germany) and TRIzol LS reagent (Invitrogen, Canada). The total RNA of the samples was quantified using NanoDropTM One (Thermo Fisher Scientific, USA) to detect concentration and purity. The total RNA system was then incubated at 25℃ for 5 min, 42℃ for 60 min, and 70℃ for reverse transcription into cDNA using a reverse transcription kit (Thermo Fisher Scientific, MA, USA). All steps were followed under the reagent manufacturer's instructions.

2.4 Quantitative real-time polymerase chain reaction (qRT-PCR)

The expression levels of hsa_circ_0023179 in different samples were detected by qRT-PCR. The primers were synthesized by Sangon Biotech Corporation (Shanghai, China). (hsa_circ_0023179 forward primer was 5-GCTCCCTTGGAAAACTGGA-3, and the reverse primer was 5-TTGGACCCCGCTCACGGCCT-3). SYBR Green I MIX (Roche), upstream/downstream primers, and ddH_2O were formulated into a 20ul system. Using 18S as an internal reference, cDNA was amplified on Roche Lightcycler 480 (Roche, Switzerland) through 45 cycles. The amplification procedure included pre-denaturation at 95 ℃ for 10min; 95 ℃ for 15 s; 58 ℃ for 30 s; 72 ℃ for 30 s. Finally, $2^{-\triangle\triangle ct}$ method was used to calculate the relative expression level of the target gene.

2.5 Detection of CEA, SCC, and Cyfra21-1 levels

ARCHITECT I2000 SR (Abbott, Chicago, USA) was used to measure serum CEA, SCC, and Cyfra21-1 levels in NSCLC patients□BPD patients and healthy donors. CEA: 0–5 ng/ mL; SCC: 0-1.5 ng/ml; Cyfra21-1:0-2.08 ng/ml is the reference range for subsequent information processing.

2.6 RNase R and Actinomycin D Assays

Ribonuclease R (RNase R, 3-4U/mg) was produced by Geneseed Biotech Co., Ltd (Guangzhou, China). RNase R, cell (A549 and NCI-H1299) RNA, 2μl RNase R buffer and enzyme-free water constitute the 20μl system. After treatment at 37℃ for 3 min, RNase R was inactivated at 70℃ for 10 min. This system is then used for reverse transcription. Actinomycin D was diluted to 2.5ug/ ml using the complete medium and added to six-well plates containing the A549 cell line at 2ml per well. After culturing for 0h, 2h, 4h, 8h, 12h, and 24h, cell RNA was extracted by trypsin digestion centrifugation.

2.7 Nucleoplasm Separation Assay

Nuclear cytoplasmic isolation of NSCLC cell lines (NCI-H1299 and NCI-H226) was performed using PARISTM Kit (Thermo Fisher Scientific). Cells were collected and rinsed with PBS before manipulation on ice. Cells were resuspended with precooled cell isolation buffer and incubated on ice for 5–10 min. Carefully separate cytoplasmic RNA and nuclear RNA after centrifugation at 500g for 3 minutes at 4°C. Then add 400μL of precooled cell destruction buffer and an equal amount of 2× Lysis/Binding Solution. Mix at room temperature, add 400μL Ethanol absolute (ACS Grade), and mix thoroughly. Pump the sample mixture through the filter element. They were washed, centrifuged, filtered, and RNA washed twice with 95℃ eluate. At last, the isolated nuclear RNA and cytoplasmic RNA were frozen at -80℃.

2.8 Statistical Analysis

SPSS 20.0 (SPSS Inc., Chicago, IL, USA) software was used for statistical analysis. Graphpad Prism 8.0 (Graphpad Software Inc., California, USA) for mapping. Paired T-Test was used to compare the differences between cancer tissues and adjacent groups. A two-sided unpaired test was used for comparing two independent samples, and one independent sample was compared by ANOVA one-way. Using ROC curve and area under the curve (AUC) to assess the diagnostic efficacy of serum hsa_circ_0023179 in NSCLC. The chi-square test analyzed the relation between hsa_circ_0023179 and pathological parameters. (*P < 0.05；**P < 0.01；***P < 0.001；****P < 0.0001；NS means no statistically difference).

3. Results

3.1 Essential Information and Characteristics of hsa_circ_0023179

High-throughput sequencing was carried out on three pairs of NSCLC tissues and their matched noncancerous tissues to investigate differentially expressed circRNAs (**Online Resource**). To express multiple of difference > 2.0 and P values < 0.05 was selected as the screening criterion, and hsa_circ_0023179 was selected for a follow-up study in combination with the analysis of CircBase, CircInteractome, and CircBank databases. hsa_circ_0023179 is present in CHR11: 68115314-68115711+, with a mature transcript length of 397 bp, according to the Ensembl Genome Database (http://www.ensembl.org). CircPrimer program revealed that hsa_circ_0023179 was made up of exon 2 reverse splicing. (Fig. 1a).

A divergent primer that can reverse amplify the circular molecule was constructed using the hsa_circ_0023179 cyclization site. The PCR amplification product of hsa_circ_0023179 was recognized with 2 percent AGE, and the electrophoresis band was 152 bp, which corresponded to the length of the primer amplification product, supporting the amplification product's accuracy (Fig. 1b). Sanger sequencing further proved that the sequence of PCR product in accord with hsa_circ_0023179, and its cyclization site was also identified (Fig. 1c). In addition, the 12 pairs of NSCLC tissues and their adjacent normal tissues collected proved that hsa_circ_0023179 was upregulated in NSCLC (Fig. 1d). In order to investigate whether serum hsa_circ_0023179 was released from NSCLC cells, cell cultures of human bronchial epithelioid cells (HBE) and NSCLC cell lines including NCI-H226, NCI-H1299, and A549. It showed that, with the extension of culture time, the content of hsa_circ_0023179 in the cellular supernatant of NCI-H226 and NCI-H1299 increased gradually (Fig. 1e), indicating that hsa_circ_0023179 may well be released into peripheral circulation from some NSCLC cell lines. Next, we verify the ring properties of hsa_circ_0023179. The circular structure of circRNA makes it more stable. Therefore, cells of NCI-H1299 and A549 were treated by RNase R, then the result was as expected. Transcriptional gene LRP5 was severely degraded than hsa_circ_0023179 (Fig. 1f), indicating the excellent stability of hsa_circ_0023179. Since RNA synthesis can be restrained by actinomycin D, A549 cell line were cultured in the actinomycin D medium. The relative expressions of hsa_circ_0023179 and transcription gene LRP5 were detected by qRT-PCR at the corresponding time nodes. It turned out that after actinomycin D treatment, hsa_circ_0023179 has a longer half-life (Fig. 1g). This section describes that hsa_circ_0023179 has the essential characteristics of circRNA.

3.2 Methodological Evaluation of hsa_circ_0023179

Next, we evaluated the detection method of hsa_circ_0023179. To test the linear range of hsa_circ_0023179 and 18S rRNA, we conducted qRT-PCR after a 10-fold dilution of cDNA from serum samples of NSCLC patients and drew standard curves according to cycle threshold (CT) values. The standard curve of hsa_circ_0023179 was y = -3.596x + 19.58, R^2 = 0.9925. And the standard curve of 18S rRNA was y = -3.521x + 10.69, R^2= 0.9944, indicating good linearity (Fig. 2a). Next, the pooled serum was room-temperature treated for 0, 6, 12, 18, and 24h, as well as repeated freeze-thaw 0, 1, 3, 5 and 10 times, respectively. The outcome showed no statistically significant change in the relative expression of hsa_circ_0023179 (P > 0.05), indicating that the test method of

hsa_circ_0023179 had satisfactory stability and repeatability (Fig. 2b, c). The qRT-PCR assay detected hsa_circ_0023179 and 18S rRNA with single peak specificity of the melting curve (Fig. 2d), and the specificity met the requirements. Briefly, the detection method of hsa_circ_0023179 is under the requirements.

3.3 Serum hsa_circ_0023179, CEA, SCC, and Cyfra21-1 Expressions

Since the stability of circRNA has been demonstrated, we intend to prove whether hsa_circ_0023179 is also stably present in serum, thus serving as a possible predictor. Serum and information were gathered from 126 NSCLC patients, 36 BPD patients, and 114 healthy subjects. The expressions of hsa_circ_0023179, CEA, SCC, and Cyfra21-1 were detected in NSCLC patients, BPD patients, and healthy subjects, respectively. qRT-PCR demonstrated that NSCLC patients' serum had higher relative expression of hsa_circ_0023179 than healthy donors ($P < 0.0001$) and BPD patients ($P < 0.0001$) (Fig. 3a). Meanwhile, CEA, SCC and Cyfra21-1 levels were also raised in NSCLC patients (Fig. 3b-d). However, in comparison with traditional detection markers, hsa_circ_0023179 showed apparent superiority in distinguishing NSCLC from BPD, implying that hsa_circ_0023179 could be exploited as an exceptional diagnostic indicator in NSCLC.

3.4 Diagnostic Value and Correlation with NSCLC Clinicopathological Parameters of hsa_circ_0023179

Compared with other mature serum markers of NSCLC, the diagnostic efficacy of hsa_circ_0023179 is an essential factor to determine whether it has the potential to be employed as a novel serum marker. ROC curves were drawn based on the expression levels of hsa_circ_0023179, CEA, SCC, and Cyfra21-1 in 126 NSCLC sufferers and 114 health volunteers, and it was found that hsa_circ_0023179 had the highest diagnostic efficiency. The areas under the curve were 0.831, 0.784, 0.431, and 0.539, respectively (Fig. 4a). hence, hsa_circ_0023179 as a serum marker of NSCLC has a potential diagnostic value. When hsa_circ_0023179 was coupled with other NSCLC serum biomarkers, the AUC was higher than that of hsa_circ_0023179 alone. When the four were diagnosed together, the most noteworthy AUG was 0.914 (Fig. 4b-d), maximizing the diagnostic value, thus revealing that hsa_circ_0023179 had higher sensitivity (SEN), specificity (SPE), total accuracy (ACCU), positive predictive value (PPV) and negative predictive value (NPV) than CEA, SCC, and Cyfra21-1, while the index was improved after the combination of four tumor markers (Table 1). In short, hsa_circ_0023179 has certain superiorities as a tumor marker, and the combined diagnosis of four biomarkers has more tremendous benefits in the diagnosis of NSCLC.

To further investigate whether hsa_circ_0023179 was associated with malignant progression of NSCLC, we collected clinicopathological data from 126 NSCLC patients. Analysis revealed that high serum hsa_circ_0023179 expression was linked to histological staging ($P = 0.0323$), TNM stage ($P = 0.031$), lymph node metastasis ($P = 0.018$) and distal metastasis ($P = 0.003$). No correlation was found with gender, age, smoking history, tumor size, etc. It is noteworthy that the levels of hsa_circ_0023179 in serum was connected with CEA ($P = 0.003$) and SCC ($P = 0.060$) (Table 2), thus providing another basis for hsa_circ_0023179 as a serum marker of NSCLC.

Table 1

Use the expression levels of hsa_circ_0023179, CEA, SCC and Cyfra21-1 to distinguish NSCLC patients from healthy donors.

	SEN	SPE	ACCU	PPV	NPV
hsa_circ_0023179	0.77(97/126)	0.86(98/114)	0.81(195/240)	0.86(97/113)	0.77(98/127)
CEA	0.39(49/126)	0.81(92/114)	0.59(141/240)	0.69(49/71)	0.54(92/169)
SCC	0.17(22/126)	0.97(107/114)	0.55(129/240)	0.88(22/29)	0.52(107/211)
Cyfra21-1	0.21(33/126)	0.98(94/114)	0.58(127/240)	0.93(33/53)	0.53(94/187)
hsa_circ_0023179+CEA	0.86(108/126)	0.87(99/114)	0.86(207/240)	0.88(108/123)	0.85(99/117)
hsa_circ_0023179+SCC	0.89(112/126)	0.87(98/114)	0.86(210/240)	0.88(112/128)	0.85(98/112)
hsa_circ_0023179+Cyfra21-1	0.77(97/126)	0.86(98/114)	0.81(195/240)	0.86(97/113)	0.77(98/127)
hsa_circ_0023179+CEA+SCC	0.86(108/126)	0.89(102/114)	0.88(210/240)	0.90(108/120)	0.85(102/120)
hsa_circ_0023179+CEA+Cyfra21-1	0.86(108/126)	0.87(99/114)	0.86(207/240)	0.88(108/123)	0.85(99/117)
hsa_circ_0023179+SCC+Cyfra21-1	0.77(97/126)	0.85(97/114)	0.81(194/240)	0.85(97/114)	0.77(97/126)
hsa_circ_0023179+CEA+SCC+Cyfra21-1	0.87(109/126)	0.89(102/114)	0.88(211/240)	0.90(109/121)	0.86(102/119)

Abbreviations:SEN, sensitivity; SPE, specificity; ACCU, overall accuracy; PPV, positive predictive value; NPV, negative predictive value.

Table 2
The correlation between hsa_circ_0023179 expression levels and clinicopathologic parameters of NSCLC patients.

Characteristics	Total	hsa_circ_0023179		P value
		High expression n = 63	Low expression n = 63	
Gender				0.212
Male	61	34	27	
Female	65	29	36	
Age (years)				0.210
≥60	57	32	25	
<60	69	31	38	
Smoking status				0.705
Non-smoker	84	41	43	
Former or current smoker	42	22	20	
Histology				0.0323*
Adenocarcinoma	110	59	51	
Squmous cell carcinoma	16	4	12	
Tumor size				0.752
≤ 5cm	115	57	58	
>5cm	11	6	5	
TNM stage				0.031*
I + II	72	30	42	
III + IV	54	33	21	
Lymph node metastasis				0.018*
Negative	90	39	51	
Positive	36	24	12	
Distant metastasis				0.003**
Negative	89	37	52	
Positive	37	26	11	
CEA				0.003**
Negative	78	31	47	
Positive	48	32	16	
SCC				0.060*
Negative	104	48	56	
Positive	22	15	7	
Cyfra21-1				0.320
Statistical analyses were carried out using Pearson χ^2 test.				
*P < 0.05, **P < 0.01 was considered significant.				

Characteristics	Total	hsa_circ_0023179		P value
		High expression n = 63	Low expression n = 63	
Negative	91	43	48	
Positive	35	20	15	
Statistical analyses were carried out using Pearson χ^2 test.				
*P < 0.05, **P < 0.01 was considered significant.				

3.5 Role of hsa_circ_0023179 in NSCLC Dynamic Monitoring

Since hsa_circ_0023179 is up-regulated in NSCLC patients, we wanted to confirm whether the expression level of hsa_circ_0023179 changes after lesion site resection in NSCLC patients, so as to validate whether hsa_circ_0023179 can be applied in real-time monitoring of NSCLC. During the experiment, the expression level of serum hsa_circ_0023179 in 24 NSCLC patients was dynamically monitored before and after surgery, and the postoperative expression level was meaningfully lower than preoperative (P = 0.0015) **(**Fig. 5a**)**, indicating that hsa_circ_0023179 has a specific potential for dynamic monitoring. Furthermore, as shown in Fig. 5b, high hsa_circ_0023179 expression was linked to a poor prognosis in a Kaplan-Meier survival curve (P = 0.0149).

3.6 Forecast for the downstream of hsa_circ_0023179 in NSCLC

To further research the mechanism of hsa_circ_0023179 in NSCLC cells, HBE was used as a normal control in NSCLC cell lines (A549, NCI-H1299, NCI-H226, and SPC-A1). The expression of hsa_circ_0023179 in these cell lines was upregulated to varying degrees (**Figure 6a)**. Nucleo-cytoplasmic separation assay demonstrated that hsa_circ_0023179 was slightly higher in the cytoplasm than that in the nucleus **(Figure 6b)**, suggesting that it may play a post-transcriptional regulatory function. Furthermore, the downstream microRNAs (miRNA) were predicted by searching bioinformatics databases (circAltas, circBank, starBase, and TargetScan). Then, the miRDB, MirPathDB, miRWalk and TargetScan databases were exploited to analyze the possible downstream mRNAs of these microRNAs. circRNA - miRNA - mRNA axes were mapped using the Cytoscape software **(Figure 6c)**, offering a new direction for the subsequent research on hsa_circ_0023179.

4. Discussion

According to global cancer statistics released by the World Health Organization (WHO) in 2020, lung cancer, the leading cancer worldwide, accounts for 11.4% of all cases (Sung et al., 2021). Although carcinogenic factors such as smoking have been controlled, primary lung cancer remains one of the most common malignancies in China. In addition to traditional surgical treatment, in recent years, the research on targeted therapies and immune checkpoint inhibitors has advanced rapidly, and the development and marketing of related drugs have changed the treatment prospects of lung cancer. Unfortunately, most patients are discovered at a late stage or with metastasis, which seriously affects the prognosis (Barash, Peled, Hirsch, & Haick, 2009). It is reported that if lung cancer can be found in time, the 5-year survival rate of patients could reach 36%-70% (Gatteschi, Iannopollo, & Gonfiotti, 2021). Currently, early detection methods of lung cancer mainly include chest X-ray, bronchoscopy, sputum analysis, cytology analysis, and low dose computed tomography (LDCT). Nevertheless, these methods have some limitations and cannot meet our expectations. Nanotechnology has revolutionized the outlook for lung cancer detection and treatment vectors in recent years. However, its immunogenicity, clearance rate, drug-carrying capacity, and targeting create obstacles and challenges for drug transformation into

the lung (S. Li et al., 2021; Srinivasan, Rajabi, & Mousa, 2015). In consequence, it's urgent for better, cheaper, less invasive, and more widespread early lung cancer detection (Haince et al., 2022).

circRNAs are a newly discovered class of RNAs that have re-entered the limelight in recent years due to their critical regulatory roles in the onset and progression of several illnesses. Exploring the expression profiles of circRNAs in tissues and cell lines of different cancer species has led to the discovery of an increasing number of differentially expressed circRNAs, owing to the rapid growth of high-throughput sequencing technology and bioinformatics analysis. Moreover, circRNA has many advantages over other non-coding RNAs (ncRNAs), such as being more stable than linear RNA (Shan et al., 2019), having higher abundance and tissue specificity (Memczak et al., 2013). Thus, circRNAs can be stably present at high levels in body fluids such as serum, urine, and exosomes. Besides, growing evidence also demonstrated the important biological functions of circRNAs (L. L. Chen, 2020; Kristensen et al., 2019). The majority of functional studies have shown that circRNAs contain miRNA response elements (MREs) to act as miRNA sponges. For instance, Li et al. found that circMAT2B activates the circMAT2B/miR-338-3p/PKM2 axis under hypoxic conditions via the sponge miR-338-3p to promote glycolysis and hepatocellular carcinoma malignancy (Q. Li et al., 2019). Besides, some articles confirmed that circRNAs could interact with RNA-binding proteins (RBP) such as circBACH1. It interacts with HuR to promote HuR translocation and facilitates its accumulation in the cytoplasm, thereby downregulating p27 expression (Kullmann, Göpfert, Siewe, & Hengst, 2002). What's more, circRNAs regulate gene transcription. For example, CircSMARCA5 terminates transcription on exon 15 of SMARCA5 by r-loop formation and upregulates truncated non-functional isoforms (Xu et al., 2020). circRNAs have been thought to be ncRNAs with regulatory roles (C. Y. Chen & Sarnow, 1995). Later, scientists have discovered translatable circRNAs (Pamudurti et al., 2017). circ β-catenin, for instance, was identified to be a protein-coding circRNA, whose translation can induce the progression of HCC by activating the Wnt pathway (Liang et al., 2019).

hsa_circ_0023179 was derived from LRP5 and obtained by circRNA high-throughput sequencing of 3 pairs of NSCLC tissues. It was remarkably upregulated in NSCLC tissues in 12 pairs of NSCLC tissues. First, AGE and Sanger sequencing were used to check that the qRT-PCR product was specific and accurate. The stability of the molecule was identified by the exonuclease digestion experiment assay and actinomycin D assay. Besides, the detection method of hsa_circ_0023179 was evaluated. The linearity and precision of CT values of qRT-PCR products met the requirements. The stability and reproducibility of qRT-PCR were recognized by placement at room temperature and multiple freeze-thaw experiments. The single specific melting curve illustrates the qRT-PCR specificity. After validation, an extensive sample analysis found that hsa_circ_0023179 was overexpressed in the serum of NSCLC patients, and the difference was remarkable compared with healthy donors and BPD patients. Subsequently, the results of ROC curve analysis indicated that hsa_circ_0023179 had higher diagnostic efficacy than CEA, SCC, and Cyfra21-1, while the combination remarkably improved the diagnostic value. In addition, high serum hsa_circ_0023179 expression was correlated with histologic type, TNM stage, lymph node metastasis, and distal metastasis, according to an analysis of clinicopathological data from 126 NSCLC patients. Furthermore, hsa_circ_0023179 expression levels decreased in NSCLC patients after surgery and had a higher survival curve in healthy subjects, suggesting the potential of hsa_circ_0023179 for dynamic monitoring. To verify whether hsa_circ_0023179 was secreted by tumor cells, we examined its expression in NSCLC cell lines (A549, NCI-H1299, NCI-H226, and SPC-A1) and discovered that all were differentially upregulated. Nucleoplasmic separation experiments demonstrated that hsa_circ_0023179 was slightly higher in the cytoplasm than in the nucleus. And in the cytoplasm, some circRNA plays a role in competing for endogenous RNA (ceRNAs) (Salmena, Poliseno, Tay, Kats, & Pandolfi, 2011). We further predicted the hsa_circ_0023179-miRNA-mRNA. Among these predicted miRNAs, hsa-miR-4644 was upregulated in plasma exosomes of bladder cancer patients and promoted bladder cancer progression by targeting UBIAD1 (Pang et al., 2021). hsa-miR-623 was confirmed to be downregulated in lung adenocarcinoma and inhibited lung adenocarcinoma growth and metastasis through ERK/JNK inactivation-mediated MMP-2/9 downregulation (Wei et al., 2016), suggesting that different regulatory networks in NSCLC progression, in which hsa_circ_0023179 may be involved.

Besides, it is worth mentioning that an increasing number of chemotherapeutic agents have been approved by FDA for the clinical treatment of lung cancer. For example, Gefitinib, Crizotinib, and Atezolimumab are important first-line therapeutic agents for lung adenocarcinoma, which inhibit the function of epidermal growth factor receptor (EGFR), mesenchymal lymphoma kinase (ALK) and programmed death-ligand 1 (PDL-1), respectively (Mottaghitalab, Farokhi, Fatahi, Atyabi, & Dinarvand, 2019). However, the resulting drug-resistant mutations are another major problem. Based on this, whether hsa_circ_0023179 plays a role in NSCLC chemotherapeutic drug resistance process may be our next exploration direction. Taken together, this study identified the upregulated hsa_circ_0023179 in NSCLC firstly by circRNA high-throughput sequencing and explored its potential as a tumor marker. However, this study also has some limitations. For instance, all samples were from Nantong University Hospital and Nantong

University Cancer Hospital, and the specimens had a certain contingency. In addition, more studies are needed to confirm whether hsa_circ_0023179 can be truly useful in the clinical setting due to the lack of standardized protocols. In summary, the high expression of hsa_circ_0023179 may serve as a potential NSCLC diagnostic marker. Nevertheless, the role of hsa_circ_0023179 in NSCLC biological regulation remains unclear. According to the analysis of hsa_circ_0023179 with clinicopathological features, hsa_circ_0023179 was associated with TNM stage, lymph node metastasis, and distal metastasis, indicating that hsa_circ_0023179 may be involved in the malignant progression of cell proliferation, migration, and invasion in NSCLC, which suggests a new direction for investigation. Our subsequent research will be focus on if hsa_circ_0023179, as ceRNA, is involved in regulating NSCLC cell proliferation, metastasis, and drug resistance, and thus implying the value of hsa_circ_0023179 as a potential therapeutic target for NSCLC.

Declarations

Funding

This project was supported by the National Natural Science Foundation of China (Grant number [81871720] and [82072363]), Graduate Research and Innovation Projects of Jiangsu Province (Grant number [KYCX21_3116]).

Conflict of interest

The authors have no relevant financial or non-financial interests to disclose.

Author Contributions

All authors contributed to the study. Qi Zhang performed the experiences and wrote the manuscript; Shiyi Qin performed the experiences and participated in the revision of the article. Chunlei Peng and Yupeng Liu provided specimens and assistance for the project. Resources and guidance for the paper were provided by Yuejiao Huang and Shaoqing Ju.

Data Availability

The datasets generated during and/or analysed during the current study are available from the corresponding author on reasonable request.

Ethics approval

All the experiments involving human participants were approved and supervised by the Ethics Committee of Affiliated Hospital of Nantong University (ethical review report number: 2018-L055).

Consent to participate

Informed consent was obtained from all individual participants included in the study.

Consent to publish

Not applicable.

References

1. Arnaiz, E., Sole, C., Manterola, L., Iparraguirre, L., Otaegui, D., & Lawrie, C. H. (2019). CircRNAs and cancer: Biomarkers and master regulators. *Semin Cancer Biol, 58*, 90-99. doi:10.1016/j.semcancer.2018.12.002
2. Barash, O., Peled, N., Hirsch, F. R., & Haick, H. (2009). Sniffing the unique "odor print" of non-small-cell lung cancer with gold nanoparticles. *Small, 5*(22), 2618-2624. doi:10.1002/smll.200900937
3. Cai, B., Ma, M., Zhou, Z., Kong, S., Zhang, J., Zhang, X., & Nie, Q. (2022). circPTPN4 regulates myogenesis via the miR-499-3p/NAMPT axis. *J Anim Sci Biotechnol, 13*(1), 2. doi:10.1186/s40104-021-00664-1
4. Cancer, I. A. f. R. o. (2020, accessed Jan 19, 2020). Global Cancer Observatory: cancer today. Retrieved from https://gco.iarc.fr/today/

5. Chen, C. Y., & Sarnow, P. (1995). Initiation of protein synthesis by the eukaryotic translational apparatus on circular RNAs. *Science, 268*(5209), 415-417. doi:10.1126/science.7536344
6. Chen, L. L. (2020). The expanding regulatory mechanisms and cellular functions of circular RNAs. *Nat Rev Mol Cell Biol, 21*(8), 475-490. doi:10.1038/s41580-020-0243-y
7. Cocquerelle, C., Mascrez, B., Hétuin, D., & Bailleul, B. (1993). Mis-splicing yields circular RNA molecules. *Faseb j, 7*(1), 155-160. doi:10.1096/fasebj.7.1.7678559
8. de Fraipont, F., Gazzeri, S., Cho, W. C., & Eymin, B. (2019). Circular RNAs and RNA Splice Variants as Biomarkers for Prognosis and Therapeutic Response in the Liquid Biopsies of Lung Cancer Patients. *Front Genet, 10*, 390. doi:10.3389/fgene.2019.00390
9. Gatteschi, L., Iannopollo, M., & Gonfiotti, A. (2021). Neoadjuvant Immunotherapy in Resectable Non-Small Cell Lung Cancer. A Narrative Review. *Life (Basel), 11*(10). doi:10.3390/life11101036
10. Haince, J. F., Joubert, P., Bach, H., Ahmed Bux, R., Tappia, P. S., & Ramjiawan, B. (2022). Metabolomic Fingerprinting for the Detection of Early-Stage Lung Cancer: From the Genome to the Metabolome. *Int J Mol Sci, 23*(3). doi:10.3390/ijms23031215
11. Herbst, R. S., Morgensztern, D., & Boshoff, C. (2018). The biology and management of non-small cell lung cancer. *Nature, 553*(7689), 446-454. doi:10.1038/nature25183
12. Kristensen, L. S., Andersen, M. S., Stagsted, L. V. W., Ebbesen, K. K., Hansen, T. B., & Kjems, J. (2019). The biogenesis, biology and characterization of circular RNAs. *Nat Rev Genet, 20*(11), 675-691. doi:10.1038/s41576-019-0158-7
13. Kullmann, M., Göpfert, U., Siewe, B., & Hengst, L. (2002). ELAV/Hu proteins inhibit p27 translation via an IRES element in the p27 5'UTR. *Genes Dev, 16*(23), 3087-3099. doi:10.1101/gad.248902
14. Li, Q., Pan, X., Zhu, D., Deng, Z., Jiang, R., & Wang, X. (2019). Circular RNA MAT2B Promotes Glycolysis and Malignancy of Hepatocellular Carcinoma Through the miR-338-3p/PKM2 Axis Under Hypoxic Stress. *Hepatology, 70*(4), 1298-1316. doi:10.1002/hep.30671
15. Li, S., Xu, S., Liang, X., Xue, Y., Mei, J., Ma, Y., . . . Liu, Y. (2021). Nanotechnology: Breaking the Current Treatment Limits of Lung Cancer. *Adv Healthc Mater, 10*(12), e2100078. doi:10.1002/adhm.202100078
16. Liang, W. C., Wong, C. W., Liang, P. P., Shi, M., Cao, Y., Rao, S. T., . . . Zhang, J. F. (2019). Translation of the circular RNA circβ-catenin promotes liver cancer cell growth through activation of the Wnt pathway. *Genome Biol, 20*(1), 84. doi:10.1186/s13059-019-1685-4
17. Memczak, S., Jens, M., Elefsinioti, A., Torti, F., Krueger, J., Rybak, A., . . . Rajewsky, N. (2013). Circular RNAs are a large class of animal RNAs with regulatory potency. *Nature, 495*(7441), 333-338. doi:10.1038/nature11928
18. Mottaghitalab, F., Farokhi, M., Fatahi, Y., Atyabi, F., & Dinarvand, R. (2019). New insights into designing hybrid nanoparticles for lung cancer: Diagnosis and treatment. *J Control Release, 295*, 250-267. doi:10.1016/j.jconrel.2019.01.009
19. Palcau, A. C., Canu, V., Donzelli, S., Strano, S., Pulito, C., & Blandino, G. (2022). CircPVT1: a pivotal circular node intersecting Long Non-Coding-PVT1 and c-MYC oncogenic signals. *Mol Cancer, 21*(1), 33. doi:10.1186/s12943-022-01514-y
20. Pamudurti, N. R., Bartok, O., Jens, M., Ashwal-Fluss, R., Stottmeister, C., Ruhe, L., . . . Kadener, S. (2017). Translation of CircRNAs. *Mol Cell, 66*(1), 9-21.e27. doi:10.1016/j.molcel.2017.02.021
21. Pang, H., Liu, L., Sun, X., Xi, W., Bao, Y., Wu, L., . . . Zhao, C. (2021). Exosomes derived from colon cancer cells and plasma of colon cancer patients promote migration of SW480 cells through Akt/mTOR pathway. *Pathol Res Pract, 222*, 153454. doi:10.1016/j.prp.2021.153454
22. Salmena, L., Poliseno, L., Tay, Y., Kats, L., & Pandolfi, P. P. (2011). A ceRNA hypothesis: the Rosetta Stone of a hidden RNA language? *Cell, 146*(3), 353-358. doi:10.1016/j.cell.2011.07.014
23. Schiffman, J. D., Fisher, P. G., & Gibbs, P. (2015). Early detection of cancer: past, present, and future. *Am Soc Clin Oncol Educ Book*, 57-65. doi:10.14694/EdBook_AM.2015.35.57
24. Shan, C., Zhang, Y., Hao, X., Gao, J., Chen, X., & Wang, K. (2019). Biogenesis, functions and clinical significance of circRNAs in gastric cancer. *Mol Cancer, 18*(1), 136. doi:10.1186/s12943-019-1069-0
25. Srinivasan, M., Rajabi, M., & Mousa, S. A. (2015). Multifunctional Nanomaterials and Their Applications in Drug Delivery and Cancer Therapy. *Nanomaterials (Basel), 5*(4), 1690-1703. doi:10.3390/nano5041690
26. Sung, H., Ferlay, J., Siegel, R. L., Laversanne, M., Soerjomataram, I., Jemal, A., & Bray, F. (2021). Global Cancer Statistics 2020: GLOBOCAN Estimates of Incidence and Mortality Worldwide for 36 Cancers in 185 Countries. *CA Cancer J Clin, 71*(3), 209-249.

doi:10.3322/caac.21660

27. Wei, S., Zhang, Z. Y., Fu, S. L., Xie, J. G., Liu, X. S., Xu, Y. J., . . . Xiong, W. N. (2016). Hsa-miR-623 suppresses tumor progression in human lung adenocarcinoma. *Cell Death Dis, 7*(9), e2388. doi:10.1038/cddis.2016.260
28. Xu, X., Zhang, J., Tian, Y., Gao, Y., Dong, X., Chen, W., . . . Wei, L. (2020). CircRNA inhibits DNA damage repair by interacting with host gene. *Mol Cancer, 19*(1), 128. doi:10.1186/s12943-020-01246-x
29. Zhang, S., Li, M., Ji, H., & Fang, Z. (2018). Landscape of transcriptional deregulation in lung cancer. *BMC Genomics, 19*(1), 435. doi:10.1186/s12864-018-4828-1

Figures

Figure 1

Characteristics of hsa_circ_0023179. **(a)** Location and origin of hsa_circ_0023179. **(b)** The primer length of hsa_circ_0023179 was verified by agarose gel electrophoresis (152bp). **(c)** Identification of the cyclization site by Sanger sequencing. **(d)** 12 pairs of tissue samples to certify the up-regulation of hsa_circ_0023179 (n = 12). **(e)** Hsa_circ_0023179 was secreted into the culture medium by NCI-H226 and NCI-H1299 cells in a time-dependent manner compared to HBE. **(f)** Stability of hsa_circ_0023179 confirmed by RNase R digestion assay. **(g)** Actinomycin D assay proved the half-life of hsa_circ_0023179 in A549 cell (P<0.0001). **P<0.01, ****P<0.0001 was considered significant, NS (P>0.05) means no statistically difference.

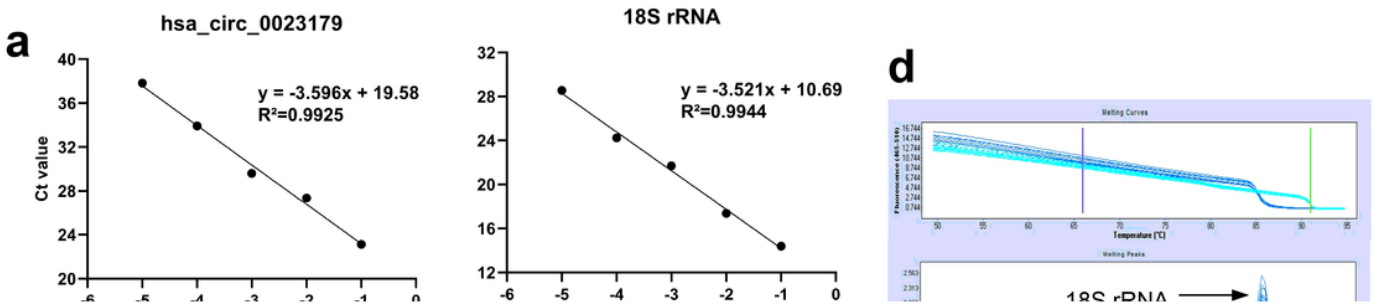

Figure 2

Methodology evaluation of hsa_circ_0023179 in NSCLC serum samples. **(a)** The linearity was showed by the standard curves of serum hsa_circ_0023179 (R^2 = 0.9925) and 18S (R^2 = 0.9944). **(b, c)** The hsa_circ_0023179 detection method was not easily influenced and had good stability and repeatability. **(d)** The PCR melting curve of hsa_circ_0023179. Abbreviations: NSCLC, non-small-cell lung cancer. NS (P>0.05) means no statistically difference.

Figure 3

Serum hsa_circ_0023179, CEA, SCC and Cyfra21-1 expressions. **(a)** Detection of serum hsa_circ_0023179 levels in NSCLC patients (n =126), healthy donors (n = 114) and BPD patients (n = 36). **(b)** Detection of serum CEA levels. **(c)** Detection of SCC levels. **(d)** Detection of serum Cyfra21-1 levels. Abbreviations: BPD, benign pulmonary disease. *P<0.05, **P<0.01, ***P<0.001, ****P<0.0001 was considered significant, NS (P>0.05) means no statistically difference.

Figure 4

Evaluation of the diagnostic value of hsa_circ_0023179 in NSCLC. **(a)** ROC analysis of independent use of serum hsa_circ_0023179, CEA, SCC and Cyfra21-1 in differentiating NSCLC patients (n = 126) from healthy donors (n = 114). **(b–d)** ROC analysis of independent/joint diagnostic efficacy of serum hsa_circ_0023179, CEA, SCC, and Cyfra21-1 in distinguishing NSCLC patients with healthy subjects. Abbreviations: ROC, receiver operating characteristic.

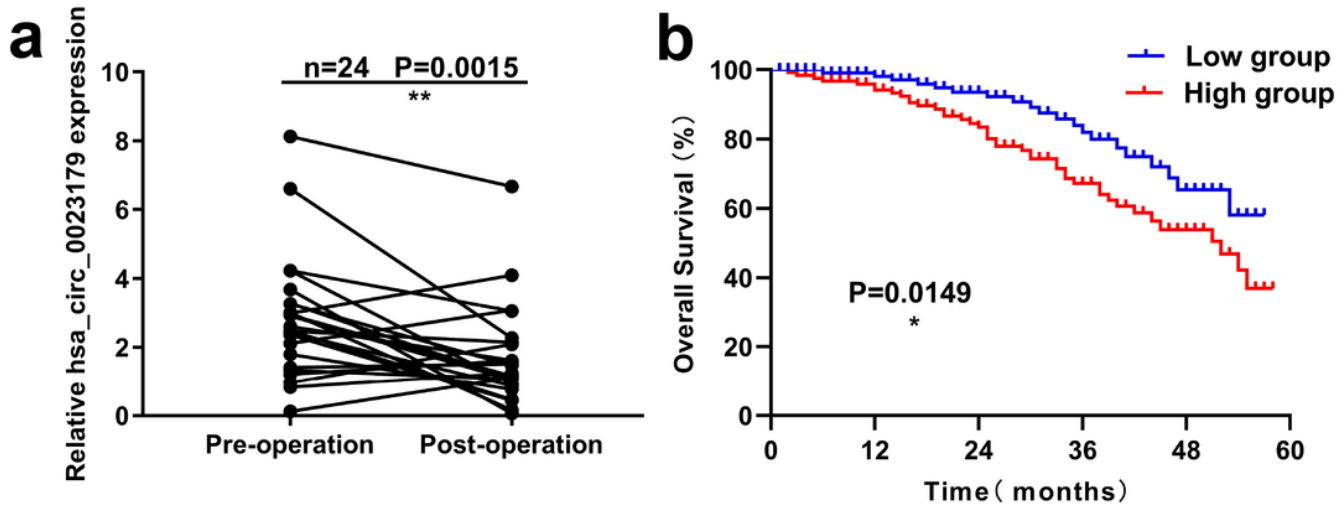

Figure 5

Role of serum hsa_circ_0023179 in monitoring tumor dynamics in NSCLC. **(a)** Altered expression of hsa_circ_0023179 in 24 paired serum samples preoperatively and postoperatively. **(b)** Kaplan-Meier survival curve analysis according to the expression levels of 126 NSCLC patients. *P<0.05, **P<0.01 was considered significant.

Figure 6

Downstream regulatory network prediction of hsa_circ_0023179. **(a)** Detection of the expression levels of hsa_circ_0023179 in four NSCLC cell lines. **(b)** The localization of hsa_circ_0023179 in NCI-H226 and NCI-H1299 cell lines was determined by nucleo-cytoplasmic separation assay. **(c)** Prediction of circRNA-miRNA-mRNA regulatory network of hsa_circ_0023179. The orange oval represents hsa_circ_0023179, and the yellow oval represents miRNAs which may bind to hsa_circ_0023179, while the blue triangle represents the target mRNA of the corresponding miRNA. *P<0.05, ***P<0.001, ****P<0.0001 was considered significant.

Supplementary Files

This is a list of supplementary files associated with this preprint. Click to download.

- SupplementaryFig.docx